REGULAR ARTICLE

blood advances

ICAM-1–targeted thrombomodulin mitigates tissue factor–driven inflammatory thrombosis in a human endothelialized microfluidic model

Colin F. Greineder,[1,*] Ian H. Johnston,[1,2,*] Carlos H. Villa,[1,3,*] Kandace Gollomp,[2] Charles T. Esmon,[4,5] Douglas B. Cines,[3] Mortimer Poncz,[1,2] and Vladimir R. Muzykantov[1]

[1]Department of Systems Pharmacology and Translational Therapeutics and [2]Division of Hematology, Department of Pediatrics, The Children's Hospital of Philadelphia, Philadelphia, PA; [3]Department of Pathology and Laboratory Medicine, Perelman School of Medicine, University of Pennsylvania, Philadelphia, PA; [4]Coagulation Biology Laboratory, Oklahoma Medical Research Foundation, Oklahoma City, OK; and [5]Department of Pathology and Department of Biochemistry and Molecular Biology, University of Oklahoma Health Sciences Center, Oklahoma City, OK

Key Points

- A microfluidic model of TF-driven thrombosis allows testing of human-specific, antibody-targeted therapeutics in whole blood under flow.
- hTM/R6.5 inhibits inflammatory thrombosis more effectively than untargeted agents (eg, shTM) and shows synergy with supplemental PC.

Diverse human illnesses are characterized by loss or inactivation of endothelial thrombomodulin (TM), predisposing to microvascular inflammation, activation of coagulation, and tissue ischemia. Single-chain antibody fragment (scFv)/TM) fusion proteins, previously protective against end-organ injury in murine models of inflammation, are attractive candidates to treat inflammatory thrombosis. However, animal models have inherent differences in TM and coagulation biology, are limited in their ability to resolve and control endothelial biology, and do not allow in-depth testing of "humanized" scFv/TM fusion proteins, which are necessary for translation to the clinical domain. To address these challenges, we developed a human whole-blood, microfluidic model of inflammatory, tissue factor (TF)–driven coagulation that features a multichannel format for head-to-head comparison of therapeutic approaches. In this model, fibrin deposition, leukocyte adhesion, and platelet adhesion and aggregation showed a dose-dependent response to tumor necrosis factor-α activation and could be quantified via real-time microscopy. We used this model to compare hTM/R6.5, a humanized, intracellular adhesion molecule 1 (ICAM-1)–targeted scFv/TM biotherapeutic, to untargeted antithrombotic agents, including soluble human TM (shTM), anti–TF antibodies, and hirudin. The targeted hTM/R6.5 more effectively inhibited TF-driven coagulation in a protein C (PC)–dependent manner and demonstrated synergy with supplemental PC. These results support the translational prospects of ICAM-targeted scFv/TM and illustrate the utility of the microfluidic system as a platform to study humanized therapeutics at the interface of endothelium and whole blood under flow.

Introduction

More than a century after the first description of purpura fulminans in 1884, the relationship between coagulation and systemic inflammation remains the subject of considerable interest and study.[1-4] The thrombotic process that occurs in the setting of infection or activation of the immune response is recognized as having distinct elements, which distinguish it from normal hemostasis or even other forms of arterial or venous thrombosis.[5] While agents such as antithrombin III and activated protein C (APC) initially held promise in treating sepsis, their clinical utility has been limited by a lack of efficacy and bleeding risks,[6,7] and the benefit of more standard anticoagulants such as heparin is uncertain.[8,9] Better understanding of the

Submitted 28 March 2017; accepted 2 July 2017. DOI 10.1182/bloodadvances.2017007229.

*C.F.G., I.H.J., and C.H.V. contributed equally to this study.

The full-text version of this article contains a data supplement.

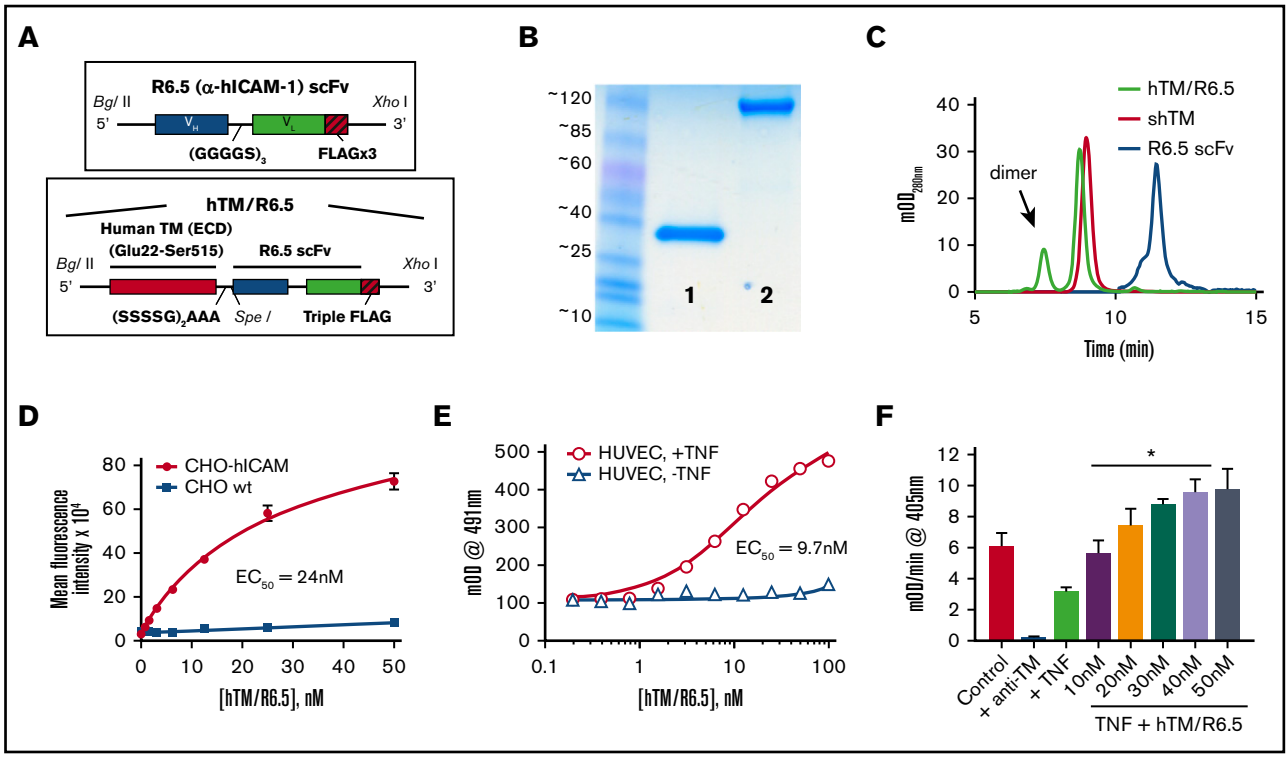

Figure 1. Assembly, characterization, and functional activity of hTM/R6.5 biotherapeutic. (A) Molecular design of R6.5 scFv and hTM/R6.5. (B) Size and purity of recombinant proteins based on sodium dodecyl sulfate-polyacrylamide gel electrophoresis (lane 1, R6.5 scFv; lane 2, hTM/R6.5) and (C) size exclusion high-performance liquid chromatography. hTM/R6.5 has a minor dimer form (indicated by arrow), accounting for ~20% of absorbance at 280 nm. (D) hTM/R6.5 binds specifically to human ICAM-1–expressing CHO cells (CHO-hICAM), but not wild type (CHO wt). Flow cytometry was performed on each cell type incubated with different concentrations of fluorescently labeled fusion protein. For each reaction, MFI was calculated for 10 000 events. Each reaction was done twice, with mean ± standard deviation (SD) of the MFI shown. (E) hTM/R6.5 binds strongly to TNF-α–stimulated HUVEC but only minimally to nonstimulated ECs. Cell-based enzyme-linked immunosorbent assays were performed on live cells as previously described[19] using anti–FLAG-HRP to probe for cell-bound fusion protein. Graph shows mean ± SD. (F) In vitro APC generation assay by cell-bound fusion protein, as described previously.[19] TNF-α–stimulated HUVECs show reduced APC generation capacity due to loss of surface TM, although some residual function is seen in comparison with cells treated with an anti-TM blocking mAb. For testing the functional activity of cell-bound hTM/R6.5, TNF-α–stimulated cells were incubated for 30 min at 37°C with various concentrations of fusion protein and then washed to remove nonspecifically bound protein prior to incubation with human thrombin (1 nM) and PC (100 nM). At saturating concentrations of hTM/R6.5 (40-50 nM), the fusion protein more than compensates for the reduction in PC activation induced by TNF-α stimulation (*$P < .01$ vs TNF only). Graph shows mean ± SD, n = 3 for each condition. EC_{50}, 50% effective concentration; mOD, 1/1000th of an optical density unit.

elements of inflammatory thrombosis and identification of targets for safe intervention represent a significant medical priority.

The protein C (PC) pathway normally functions to limit excessive activation of coagulation, but it is suppressed in the setting of systemic inflammation. Inflamed endothelial cells (ECs) demonstrate loss of the natural anticoagulants thrombomodulin (TM) and the endothelial protein C receptor (EPCR) from their luminal surface.[10-14] Conversely, tissue factor (TF) expression on a variety of cell types in systemic inflammation promotes activation of coagulation and is an attractive target for intervention.[15,16] Existing pharmacologic approaches intended to intercept inflammatory activation of coagulation may be limited by their inability to localize to TF-expressing procoagulant surfaces. For example, soluble human TM (shTM), which is currently being evaluated in a phase 3 clinical trial of patients with severe sepsis and coagulopathy (www.clinicaltrials.gov identifier #NCT0158831), lacks any specific affinity for cellular surfaces.[17]

Our laboratory has pursued a pharmacologic approach to attenuate inflammation by specifically targeting TM to activated cellular surfaces.[18] In the first report of this strategy, recombinant mouse TM was fused to a single-chain antibody fragment (scFv) specific for mouse intracellular adhesion molecule 1 (ICAM-1, or CD54). In a murine model of acute lung injury, ICAM-1–targeted scFv/TM was found to facilitate interaction with endogenous EPCR, reduce inflammatory markers, and improve transendothelial plasma protein leakage.[19] While these studies demonstrated the potential therapeutic benefit of this approach, the effect on activation of coagulation was not examined.

The challenges in demonstrating the efficacy of ICAM-1–targeted TM in TF-driven inflammatory thrombosis are several fold. First, there is uncertainty over the clinically significant sources of TF in sepsis and related disorders.[20,21] Differences in cellular sources of TF are particularly relevant to scFv/TM, as its distribution is more controlled than untargeted "fluid-phase" agents (ie, soluble TM) and therefore more likely sensitive to changes in the relative cellular contributions to thrombin generation. It is challenging to discern the contribution of endothelial TF from other sources such as hematopoietic cells, epithelium, fibroblasts, pericytes, and smooth muscle.[22-24] While ECs express TF under inflammatory stimuli in vitro, studies have failed to

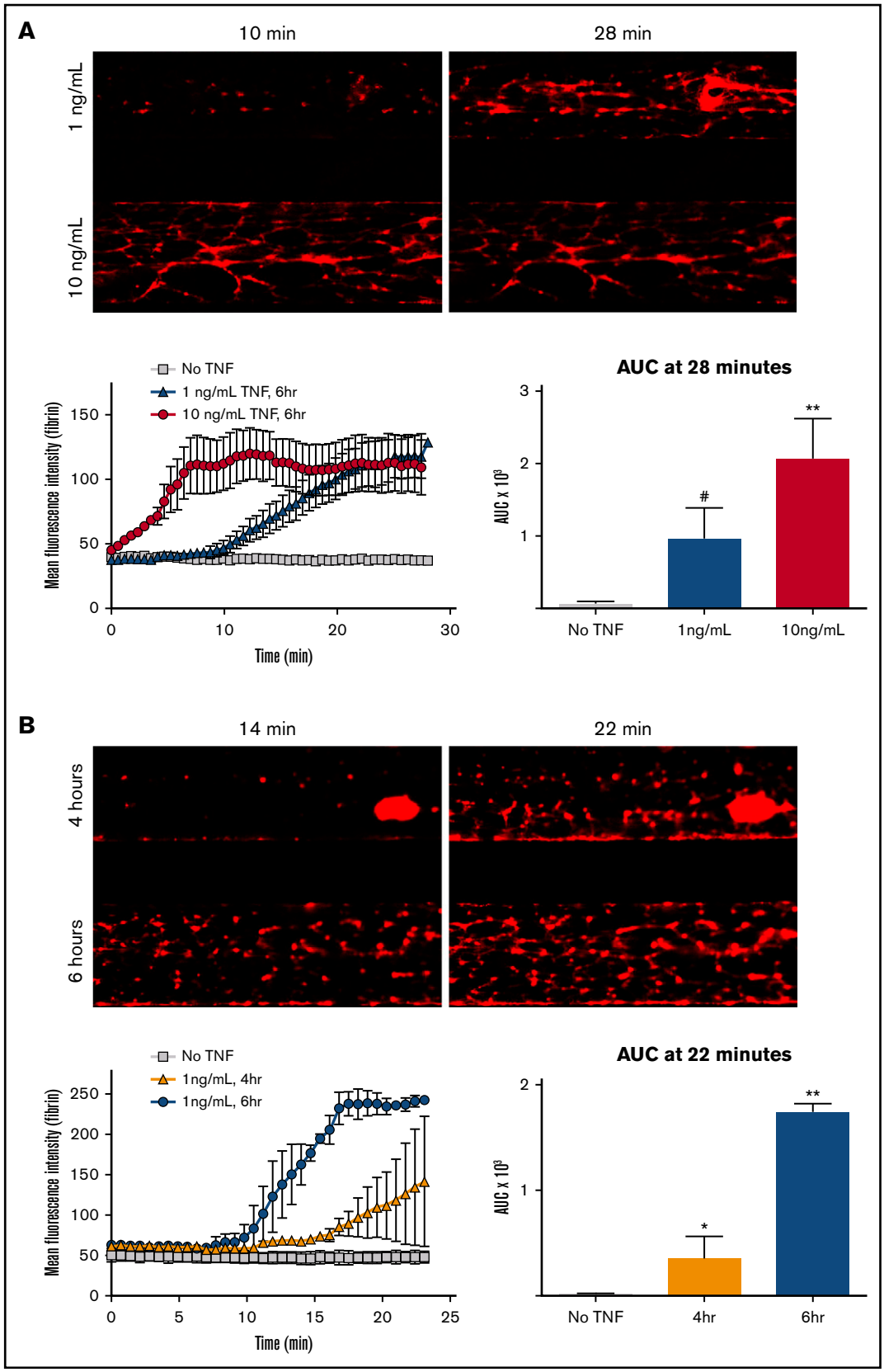
A
10 min
28 min
1 ng/mL
10 ng/mL
No TNF
1 ng/mL TNF, 6hr
10 ng/mL TNF, 6hr
Mean fluorescence intensity (fibrin)
Time (min)
AUC at 28 minutes
AUC x 10³
No TNF
1ng/mL
10ng/mL
B
14 min
22 min
4 hours
6 hours
No TNF
1ng/mL, 4hr
1ng/mL, 6hr
Mean fluorescence intensity (fibrin)
Time (min)
AUC at 22 minutes
AUC x 10³
No TNF
4hr
6hr

Figure 2.

demonstrate a definitive role of endothelial TF in murine models,[25] which may not fully replicate human biology or be sensitive to the contribution of endothelial TF to activation of coagulation.[22,24] TM itself demonstrates species-specific differences in the balance between anti-inflammatory and antithrombotic activity.[26,27] Finally, translation to human pathologies has been limited by the absence of species cross-reactivity of the murine therapeutic.

To address these challenges and provide a model that can begin to close this translational gap, we have adapted a commercially available, multichannel microfluidic system that uses human whole blood (WB) perfused through cytokine-activated, human endothelial–lined flow chambers, with real-time microscopy for visualization of underlying pathophysiologic events. We report the development and efficacy of a "humanized" scFv/TM therapeutic, hTM/R6.5, which incorporates both human TM and a human-specific anti–ICAM-1 scFv. This approach allowed testing of ICAM-1–targeted scFv/TM as an intervention in TF-driven inflammatory thrombosis using an entirely human system, employing multiple channels run simultaneously, allowing for a side-by-side comparison of therapeutic interventions within a single experiment.

Materials and methods

Venipuncture and WB preparation

All studies involving human subjects were approved by the University of Pennsylvania institutional review board (protocol 822534). Written informed consent from healthy volunteer donors was obtained for the use of deidentified blood samples. WB samples were collected from the antecubital vein using a 19G butterfly cannula system. The first 5 mL of blood was discarded, followed by collection into vacuum tubes containing citrate and corn trypsin inhibitor (CTI), with final concentrations of 11 mM and 50 μg/mL, respectively.

In experiments involving inflammatory activation of WB, 50 ng/mL lipopolysaccharide (LPS) was added for 90 minutes at 37°C. In experiments involving PC-deficient blood, WB samples were centrifuged for 15 minutes at 1500*g* at room temperature to isolate platelet-poor plasma. 50% of the original plasma was removed and replaced with an equivalent volume of PC-immunodepleted or normal control plasma. Corn trypsin inhibitor was then added to maintain the final blood concentration at 50 μg/mL.

In all experiments, 5 μg/mL Alexa Fluor 568/antifibrin monoclonal antibody (mAb) was added to WB, along with either calcein-AM (2 μg/mL) or fluorescent antileukocyte and platelet antibodies (Brilliant Violet anti-CD45 and FITC anti-CD41, each 1.5 μg/mL). WB samples were recalcified just prior to infusion into the microfluidic channels, adding $CaCl_2$ to a final concentration of 11 mM.

Microfluidic model of inflammatory thrombosis

Endothelialized microfluidic chambers were prepared by seeding human umbilical vein endothelial cells (HUVECs) into fibronectin-coated, glass-bottomed, polydimethylsiloxane (PDMS) flow chambers of high-shear, 48-well Bioflux plates (Fluxion Biosciences, San Francisco, CA). The Bioflux system uses constant pressure applied to input wells to generate flow at specified levels of shear stress.

On the day of experimentation, endothelialized channels were flow adapted for 4 to 6 hours at 5 dynes/cm^2 at 37°C. To induce inflammatory activation of ECs, tumor necrosis factor alpha (TNF-α) was added at varying concentrations during the flow adaption period. Fresh media was allowed to flow through the channels for 30 minutes to "wash out" residual TNF-α prior to introduction of WB. In some experiments, EC-targeted antibodies or recombinant proteins were added during the first 25 minutes of this washout period, followed by 5 minutes of flow to remove nonspecifically bound protein. In other experiments, antithrombotic agents were mixed into WB.

While each Bioflux 48-well plate contains 24 flow chambers, WB experiments were run with no more than 8 channels (4 pairs of 2) at once to minimize the time between imaging of each pair of channels. This setup allowed 2 or 3 replicates for each of 3 or 4 experimental conditions (eg, control, TNF-α only, TNF-α + therapeutic A, and TNF-α + therapeutic B). A computer interface was used to move a motorized microscope stage (Fluxion Biosciences) rapidly between viewing areas, allowing each pair of channels to be imaged approximately every 15 to 30 s. Imaging was performed on a Zeiss Axio Observer microscope under a 10×/0.25 objective. The focal plane was set to be at the interface of the lower wall endothelial layer and the WB. Under this objective and aperture, we expect the depth of field to be ~8.5 μm. Fluorescent images were acquired using identical settings for all channels, while bright-field images allowed direct visualization of flow.

Confocal microscopy

Channels were fixed by flowing 4% paraformaldehyde at 1 dyne/cm^2 into the channel for 15 minutes. The cells were washed with PBS and blocked with 5% donkey serum prior to adding primary and secondary antibody and staining with Hoechst reagent. Imaging was performed using a Zeiss LSM 710 at original magnification ×20.

Data analysis and statistics

Each figure represents data from a single experiment with means and standard errors derived from replicate channels within that experiment. For analyses, bright-field and fluorescence microscopy images were imported into ImageJ and analyzed frame by frame using identical acquisition parameters for each experiment. Backgrounds were subtracted using an ImageJ rolling-ball algorithm with a radius of 50 pixels. Preset regions of interest, covering the entire channel except the areas immediately adjacent to the side walls, were used to measure mean fluorescence intensity (MFI) in green and red channels or mean signal intensity in the bright-field channel. Frame "time codes" were used to generate time courses, and areas under the curve (AUCs) were calculated for statistical comparisons. First-derivative curves were calculated with statistical software (GraphPad, La Jolla, CA).

Significant differences between means were determined using Prism 6.0 software (GraphPad, La Jolla, CA). One-way analysis of variance was performed, followed by appropriate multiple comparison

Figure 2. Fibrin deposition in microfluidic model of inflammatory thrombosis. Fibrin deposition was monitored via red fluorescent antifibrin mAb during perfusion of WB through TNF-α–activated endothelialized channels at shear stress of 5 dynes/cm^2. Accumulation of fibrin varies with increasing (A) concentration (1 ng/mL vs 10 ng/mL, each for 6 hours) and (B) duration (4 hours vs 6 hours, each 1 ng/mL) of TNF-α preactivation. Left panels show representative fluorescent images at various time points. Middle panel shows MFI vs time, with mean ± standard error of the mean (SEM) shown for n = 2 channels for control (no TNF) groups and n = 3 channels for each experimental group. Right panel shows AUC analyses. *$P < .05$ vs control; **$P < .05$ vs each other condition; #, not significant ($P = .14$).

(Tukey) test and calculation of multiplicity adjusted P values. $P < .05$ was considered statistically significant.

Additional materials and methods can be found in the supplemental Material.

Results

Production and characterization of human-specific anti-ICAM scFv/TM

To create the humanized anti-ICAM scFv/TM complementary DNA (cDNA) construct (hTM/R6.5), cDNA encoding the extracellular portion of human TM (Glu22-Ser515) was fused with the R6.5 scFv cDNA, containing V_H and V_L domains cloned from the corresponding anti–human ICAM-1 hybridoma.[28,29] The detailed molecular design of each construct is shown in Figure 1A. Purified R6.5 scFv and hTM/R6.5 migrated as single bands on nonreducing sodium dodecyl sulfate-polyacrylamide gel electrophoresis (Figure 1B), with sizes (~35 kDa and ~120 kDa) similar to those seen for previous scFv and scFv/TM fusion proteins (TM runs significantly higher than its predicted size due to glycosylation). Similar purity was seen on size-exclusion high-performance liquid chromatography, although this method revealed a dimer form of hTM/R6.5, which accounted for ~20% of total absorbance (Figure 1C). As shown in Figures 1D and E, hTM/R6.5 demonstrated high affinity, specific binding to human ICAM-1 in a flow cytometry based assay with stably-transfected CHO cells (K_d = 24 nM) and a cell-based enzyme-linked immunosorbent assay on TNF-α–activated HUVECs (K_d = 9.7 nM), respectively. The fusion protein was functionally active when bound to TNF-α–activated HUVECs, demonstrating thrombin-dependent PC activation after binding and washing to remove nonspecifically bound protein. At concentrations (40-50 nM) sufficient to saturate available binding sites on these cells, the fusion protein more than compensated for the loss of APC generation caused by activation of the ECs by cytokine ($P < .01$; Figure 1F).

Establishing a multichannel system of endothelialized flow channels

To enable testing of hTM/R6.5 at the interface of human WB and endothelium, HUVECs were grown in microfluidic flow chambers until they established 3-dimensional, fully confluent, endothelialized channels (typically 2-3 days). Following 6 hours of flow adaptation at 5 dynes/cm^2, a shear stress typical of postcapillary venules,[30] cells covered all surfaces of the flow chamber (supplemental Movie 1), maintained a normal cobblestone morphology, and showed a typical pattern of PECAM-1 (CD31) expression, with staining predominantly at cell–cell junctions (supplemental Figure 1). Infusion of human WB (collected in citrate/CTI and recalcified) for up to 60 minutes did not cause deposition of fibrin, adhesion of leukocytes or platelets to ECs, or disruption of flow. The bottom panels of supplemental Movies 2 (fluorescence) and 3 (bright field) show a representative time-lapse video (each frame represents ~30 s) of ~20 minutes of blood flow through a quiescent endothelialized channel, with no accumulation of fibrin (red) or cellular adhesion (green) and no disruption of flow.

Characterization of inflammatory thrombosis model

We next sought to model the intravascular events of human inflammatory thrombosis by flowing WB through TNF-α–activated endothelialized channels. A schematic diagram of this 2-step model is shown in supplemental Figure 2A. Confocal imaging of TNF-α–activated channels showed the expected changes in luminal expression of a variety of markers, including increased TF, ICAM-1, and VCAM-1 and decreased TM (supplemental Figure 2B-D). The top panels of supplemental Movies 2 (fluorescence) and 3 (bright field) show infusion of WB into a cytokine-activated endothelialized channel that, in stark contrast to the quiescent channel, results in rapid adhesion of leukocytes and platelets, deposition of fibrin, and ultimately occlusion of flow.

To determine the optimal conditions for testing antithrombotic therapeutics, we defined the extent of coagulation in the microfluidic model as a function of the dose and time of cytokine exposure. Both higher concentration of TNF-α (Figure 2A; supplemental Movie 4) and longer duration of stimulation (Figure 2B; supplemental Movie 5) led to greater fibrin deposition upon infusion of WB. These experiments also revealed the advantage afforded by the multichannel format, which allowed comparison of multiple experimental conditions (with replicates) within a single experiment. Supplemental Figure 3 shows the relatively small variance within a single experiment, compared with the variability across experiments with separate EC preparations and WB samples. On the basis of these results, each subsequent experiment was performed with a single blood sample and EC preparation and 8 microfluidic channels. The MFI of the fibrin signal rose in roughly sigmoidal fashion with a bell-shaped first-derivative curve, analogous to a thrombin generation curve generated from thrombin generation assay (TGA) data (supplemental Figure 4).[31] Two parameters (peak fibrin generation rate and the time to peak rate) derived from these curves were found to be dependent on time and dose of TNF-α (supplemental Tables 1 and 2).

Apart from fibrin deposition, other physiologically relevant outcomes were found to vary with the extent of cytokine activation of the endothelialized channels. In particular, adhesion of leukocytes and platelets, based on accumulation of green fluorescence, was seen only after TNF-α stimulation (supplemental Figure 5A; supplemental Movie 6). Higher doses of TNF-α also demonstrated earlier disruption and occlusion of blood flow, based on changes in bright-field signal intensity (supplemental Figure 5C; supplemental Movie 8). Separately tracking platelets and leukocytes using antibodies to platelet GPIbIIIa labeled in green and antibodies to leukocyte CD45 labeled in blue, we found that while that the number of adherent platelets varied with TNF-α concentration in the range of 1 to 10 ng/mL, the number of adhered leukocytes was similar (supplemental Figures 5B and 6; supplemental Movie 7). We confirmed this finding using an automated cell counting algorithm to enumerate adherent leukocytes flowing over TNF-α–activated channels and found similar numbers of adhered leukocytes per channel area in channels treated with either 1 or 10 ng/mL TNF-α (supplemental Figure 6A). Additional experiments performed across a lower range of TNF doses (0.1-1 ng/mL) revealed a dose response of leukocyte adhesion to TNF stimulation within this lower range (supplemental Figure 6B). Finally, flowing WB over TNF-α–activated channels resulted in not only adhesion of leukocytes but also an activation of neutrophils that resulted in deposition of neutrophil extracellular traps,[32] which could be visualized in real time with nucleic acid stains (supplemental Figure 7).[33]

Inflammatory thrombosis model is TF driven

We next validated the role of TF in initiating coagulation in this model, noting that peripheral blood was collected in the presence of CTI, a factor XIIa inhibitor.[34] Figure 3A shows the experimental

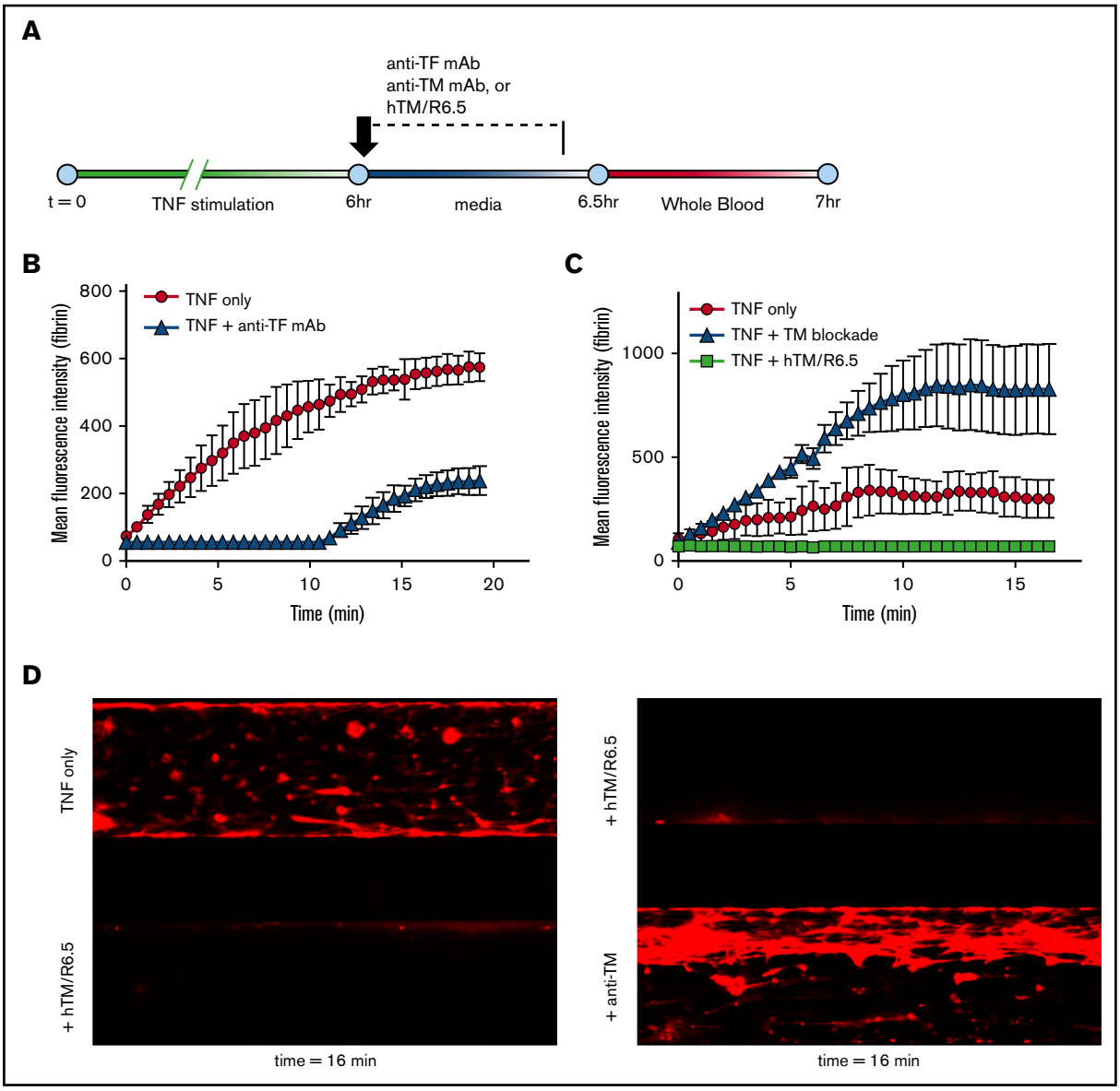

Figure 3. Endothelial TM regulates TF-driven coagulation in inflammatory thrombosis model. (A) Schematic showing experimental design. Endothelialized channels were flow adapted at shear stress of 5 dynes/cm^2, stimulated with 1 ng/mL TNF-α for 6 hours, and then treated with antibodies or fusion protein during the first 25 minutes of a 30-minute TNF-α washout period, followed by a 5-minute wash to remove nonspecifically bound protein and, finally, infusion of WB at shear stress of 5 dynes/cm^2. (B) Blockade of endothelial TF delays and markedly reduces fibrin deposition ($P = .02$ for AUC of TNF vs TNF + anti-TF mAb). Graph shows mean ± SEM, with n = 2-3 channels per condition. (C) Blockade of endothelial TM results in significant increase in fibrin deposition ($P < .001$ for AUC of TNF only vs TNF + TM blockade), whereas treatment of TNF-α–activated endothelium with hTM/R6.5 scFv fusion protein completely eliminates fibrin deposition ($P = .03$ for AUC of TNF only vs TNF + hTM/R6.5). Graph shows mean ± SEM, with n = 2-3 channels per condition. (D) Representative fluorescent images for panel C show fibrin deposition within endothelialized channels and demonstrate opposing effects of TM inhibition and augmentation.

design, in which TF inhibitory antibody (or media control) was flowed over TNF-α–activated endothelialized channels prior to the infusion of WB. As shown in Figure 3B and supplemental Movie 9, TF blockade significantly ($P = .02$) reduced fibrin deposition, confirming the role of endothelial TF as a driver of coagulation in this model. Analysis of first-derivative curves showed that anti-TF led to both a decrease in peak fibrin generation rate and an increase in the time to peak fibrin generation (supplemental Table 3). TF antibody also decreased the accumulation of green fluorescence (supplemental Figure 8A), reflecting the sum of leukocyte and platelet adhesion. While these cell types were not individually stained in this experiment, the morphology suggested a decrease in platelet rather than leukocyte adhesion.

Endothelial TM regulates inflammatory activation of coagulation

A similar approach was taken to investigate the role of endogenous endothelial TM in regulating coagulation in the WB microfluidic model. Although TNF-α stimulation decreases endothelial TM, some

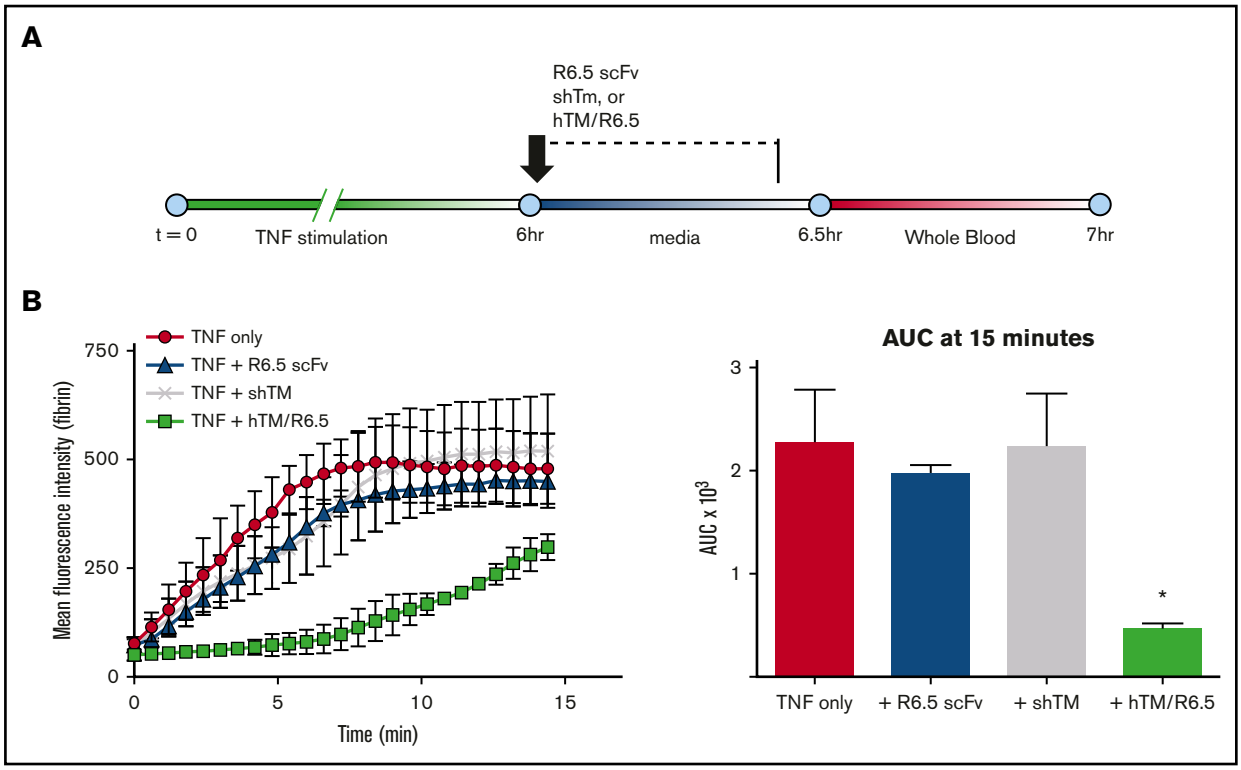

Figure 4. Both domains of hTM/R6.5 are required to generate an antithrombotic effect. (A) Experimental design. All proteins were infused in equimolar concentrations (50 nM) during the TNF washout period, followed by a 5-minute wash to remove nonspecifically bound protein. Flow of media and WB was at shear stress of 5 dynes/cm^2. (B) Only hTM/R6.5 inhibited fibrin deposition, confirming that both the ICAM-1 binding and hTM domains must be present to produce an antithrombotic effect. Left panel shows MFI vs time, mean ± SEM, with n = 2 channels per condition. Right panel shows AUC analysis. *$P < .05$ vs all other conditions.

APC generation capacity remains (Figure 1F). To achieve complete inhibition, we used an antibody specific for the fifth epidermal growth factor–like domain of TM, which blocks thrombin binding and eliminates nearly all APC generation capacity (Figure 1F).[35] Treatment of TNF-α–stimulated channels with this antibody prior to the infusion of WB significantly increased fibrin deposition ($P < .001$; Figure 3C-D). Analysis of first-derivative curves revealed an increase in the peak fibrin generation rate (supplemental Table 4).

These results established the microfluidic model as a means to test targeted therapeutics in a humanized system, with the hypothesis that the ICAM-1 targeted fusion protein would localize to activated cellular surfaces, reverse the loss of endothelial TM induced by cytokine activation, and abrogate the TF-driven thrombotic response. Indeed, treatment of TNF-α–activated endothelialized channels with 50 nM hTM/R6.5, a concentration chosen based on the prior binding studies (Figure 1E), produced the opposite effect of the TM blocking antibody, completely eliminating fibrin deposition (Figure 3B-C; supplemental Table 4; supplemental Movie 10). As seen previously, effects on green fluorescence mirrored those seen for fibrin generation, consistent with a reduction in platelet adhesion (supplemental Figure 8B; supplemental Movie 10).

Comparative testing of antithrombotic agents

Given the effectiveness of hTM/R6.5 in the WB microfluidic model, we next took advantage of the multichannel format to compare its antithrombotic efficacy with that of other antithrombotic agents. As a first step, the fusion protein was tested against equimolar concentrations of its individual components, shTM and R6.5 scFv. These proteins had minimal effects on fibrin deposition when infused during the TNF-α washout period (Figure 4; supplemental Table 5). While expected, this confirmed that both domains of the fusion protein are required for its activity and excluded that ICAM-1 blockade alone might be solely responsible for the observed antithrombotic effect.

Endothelial-bound hTM/R6.5 was next tested against shTM added directly to WB. Figure 5A shows the experimental design of these experiments. While both agents significantly decreased fibrin deposition (Figure 5B; supplemental Table 6; supplemental Movie 11), the effect of shTM was less sustained ($P = .05$), even at a dose far greater than its IC50 in TF-induced thrombin generation assays.[36] It should be noted that hTM/R6.5 was limited to the protein bound to the cells, as the targeted protein was not added to WB in these experiments. Hirudin (5 U/mL) and hTM/R6.5 (50 nM) were also compared and demonstrated similar results ($P = .03$; Figure 5C; supplemental Movie 12). Consistent with previous TGA reports,[36] hirudin primarily affected the time to peak fibrin generation, without a major effect on the peak generation rate (supplemental Table 7).

hTM/R6.5 was next compared with shTM following a combination of cytokine activation of ECs and inflammatory activation of WB (Figure 6A). The latter was induced by 90-minute preincubation of the WB with 50 ng/mL LPS, conditions previously used to induce neutrophil oxidative burst and monocyte TF expression in human WB.[37,38] LPS was chosen to better simulate human disease states, such as sepsis, in which activated leukocytes and other blood

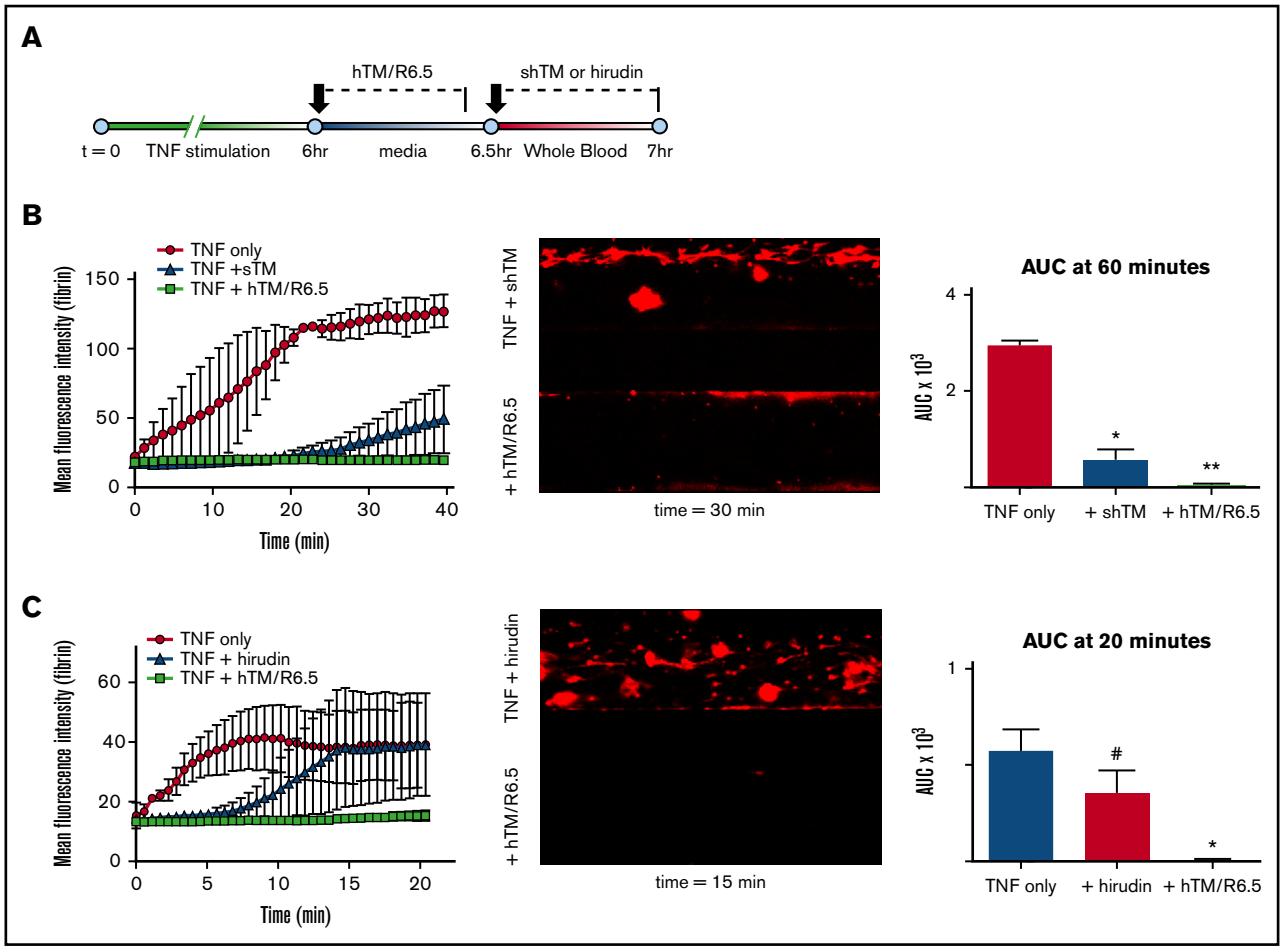

Figure 5. Comparative testing of antithrombotic agents. (A) Experimental design, showing distinct timing of treatment with hTM/R6.5 scFv, bound to ECs during the first 25 minutes of the TNF-α washout period, vs soluble agents, which were mixed into WB. (B-C) Both 100 nM shTM (B) and 5 U/mL hirudin (C) inhibited coagulation but were less effective than hTM/R6.5 (50 nM). Left panels show MFI vs time, ± SEM, with n = 2 channels for TNF-α only and n = 3 channels for each therapeutic. Middle panels show representative fluorescent images. Right panels show AUC analyses. *$P < .05$ vs TNF only; **$P < .05$ vs both other conditions; #, not significant ($P = .17$).

components may contribute to inflammatory thrombosis.[4,5] While both agents demonstrated antithrombotic effect in this setting, hTM/R6.5 was significantly more effective in inhibiting fibrin deposition than shTM ($P = .05$; Figure 6B; supplemental Table 8; supplemental Movie 13). In all experiments, the effect of hTM/R6.5 on fibrin deposition was mirrored by reduction in accumulation of green fluorescence, consistent with a decrease in platelet accumulation (supplemental Figure 8C-D; supplemental Movies 11-13).

hTM/R6.5 is at least partially PC dependent

We next tested the contribution of PC activation to the antithrombotic activity of hTM/R6.5. A recently reported antibody, HAPC1573, which binds human APC (but not its zymogen) and inhibits its inactivation of factors Va and VIIIa in a dose-dependent manner,[39] was mixed into WB (Figure 7A). In naive WB, HAPC1573 treatment produced fibrin deposition similar to equimolar isotype control antibody ($P = .33$), although shortened time to peak fibrin generation was observed (supplemental Table 9). APC inhibition markedly increased fibrin deposition in endothelialized channels treated with hTM/R6.5 ($P < .05$), although a persistent delay was seen in the time to peak fibrin generation (Figure 7B-D; supplemental Table 9; supplemental Movie 14). This effect, reported in previous TGA studies, has been attributed to direct inhibition of thrombin by TM.[36]

These results prompted investigation of hTM/R6.5 in the setting of PC deficiency, a condition observed in sepsis and other syndromes involving systemic activation of coagulation.[40-42] To achieve the levels of PC deficiency similar to patients with these illnesses, we removed 50% of the plasma from donor WB and replaced it with an equal volume of PC-immunodepleted (or nondepleted control) plasma (Figure 8A). Like APC inhibition, partial depletion of plasma PC produced fibrin deposition similar to control WB ($P = .34$), with a slight decrease in time to peak fibrin deposition.[43] PC deficiency dramatically altered the activity of the fusion protein, eliminating its inhibitory effect on overall fibrin deposition ($P = .34$; Figure 8B-D) and the decrease in peak fibrin generation rate seen in control WB (supplemental Table 10). In contrast, hTM/R6.5 produced a delay in time to peak fibrin generation in both PC-deficient and control WB, consistent with direct thrombin inhibition by the fusion protein (supplemental Table 10).[36] Finally, addition of exogenous, plasma-derived human PC to the PC-depleted blood restored the full antithrombotic effect of hTM/R6.5 ($P < .05$; Figure 8B-D; supplemental Table 10; supplemental Movie 15).

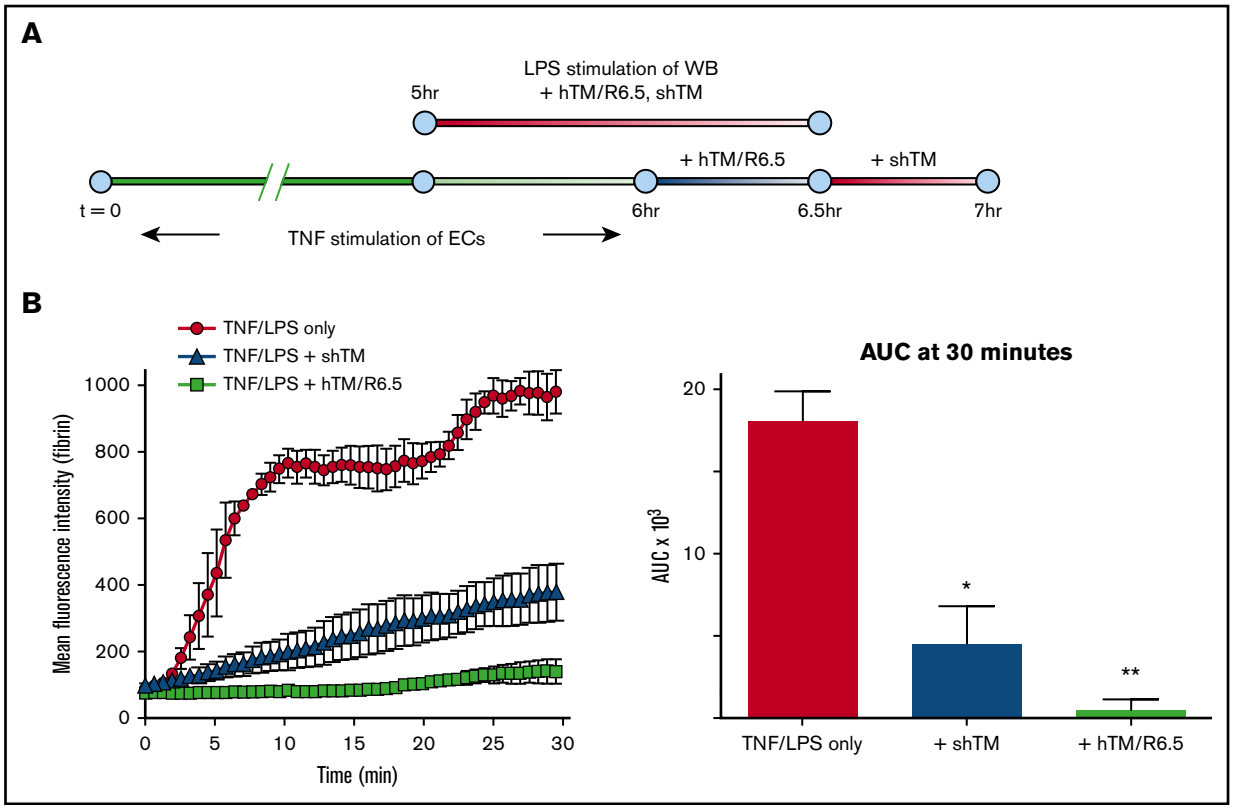

Figure 6. hTM/R6.5 has greater antithrombotic activity than shTM in combined model of endothelial cytokine activation and endotoxemia. (A) Experimental design, showing 6-hr stimulation of endothelialized channels with TNF-α and 90-minute preactivation of WB with LPS (50 ng/mL). In this case, hTM/R6.5 (50 nM) was infused during the TNF-α washout period and mixed into the WB. (B) The fusion protein provided superior antithrombotic effect. Left panels show MFI vs time, mean ± SEM, with n = 2 channels for TNF/LPS only and n = 3 channels for each therapeutic. Right panels show AUC analyses. *$P < .05$ vs TNF/LPS only; **$P < .05$ vs both other conditions.

Discussion

This is the first report of ICAM-1 targeted fusion proteins as a therapy for TF-driven inflammatory thrombosis. Affinity targeting to cellular surfaces has the potential to dramatically alter local concentrations and interaction with binding partners, particularly in surface-driven phenomena such as coagulation, and the improved efficacy of hTM/R6.5, compared with other therapeutics, including sTM, hirudin, and anti-TF, demonstrates the translational potential of this approach. hTM/R6.5 bound to the surface of activated human ECs and restored APC generation capacity above that of uninflamed endothelium. hTM/R6.5 shares a number of desirable features with its mouse-specific analog, YN1/mTM,[19] and the use of an scFv fragment enables facile genetic fusion to therapeutic cargoes and mitigates the Fc and complement-mediated toxicities seen in clinical trials of the parental antibody, R6.5, or enlimomab.[44-47]

To demonstrate the therapeutic efficacy of human-specific hTM/R6.5, a microfluidic system consisting of entirely human components was developed to model TF-driven inflammatory thrombosis. Sophisticated in vitro systems have been developed that incorporate multiple cell types and reproduce the architecture of microvascular networks.[48-52] Our priority was to establish a comparatively straightforward model, suitable for testing and comparing targeted scFv/TM with other antithrombotic drugs.[18,53-55] Although the model lacks subendothelial components of a true vessel, including epithelial tissues, it allows for control over endothelial and leukocyte activation, manipulation and treatment of human WB, and quantification of therapeutic effects with high spatial and temporal resolution. While the present focus was on abrogation of fibrin deposition, additional readouts of inflammatory biology such as leukocyte adhesion and generation of neutrophil extracellular traps were also shown to be possible using this model system. By calculating first-derivative curves of fibrin fluorescence intensity, we provide readouts analogous to common TGA assays. Importantly, the multichannel format of this system allows for parallel testing of multiple therapeutic approaches with a single blood donor and EC preparation, limiting the impact of these variables, which can complicate other complex microfluidic model systems.

Several limitations of the model should be highlighted. First, PDMS flow chambers are rectangular in cross-section and fail to reflect the mechanical compliance of normal vasculature.[56] Use of linear channels with fixed dimensions and no branches limits extrapolation to physiologic vascular beds, where inflammatory, TF-driven thrombosis may occur heterogeneously.[57] The important physiologic sources of TF are a matter of ongoing investigation,[58] and as currently constructed, this model is limited to hematopoietic and endothelial sources. In addition, only HUVEC cells were investigated in the current model, although further optimization to enable culture of and comparison with other endothelial sources is ongoing. The current conformation does not

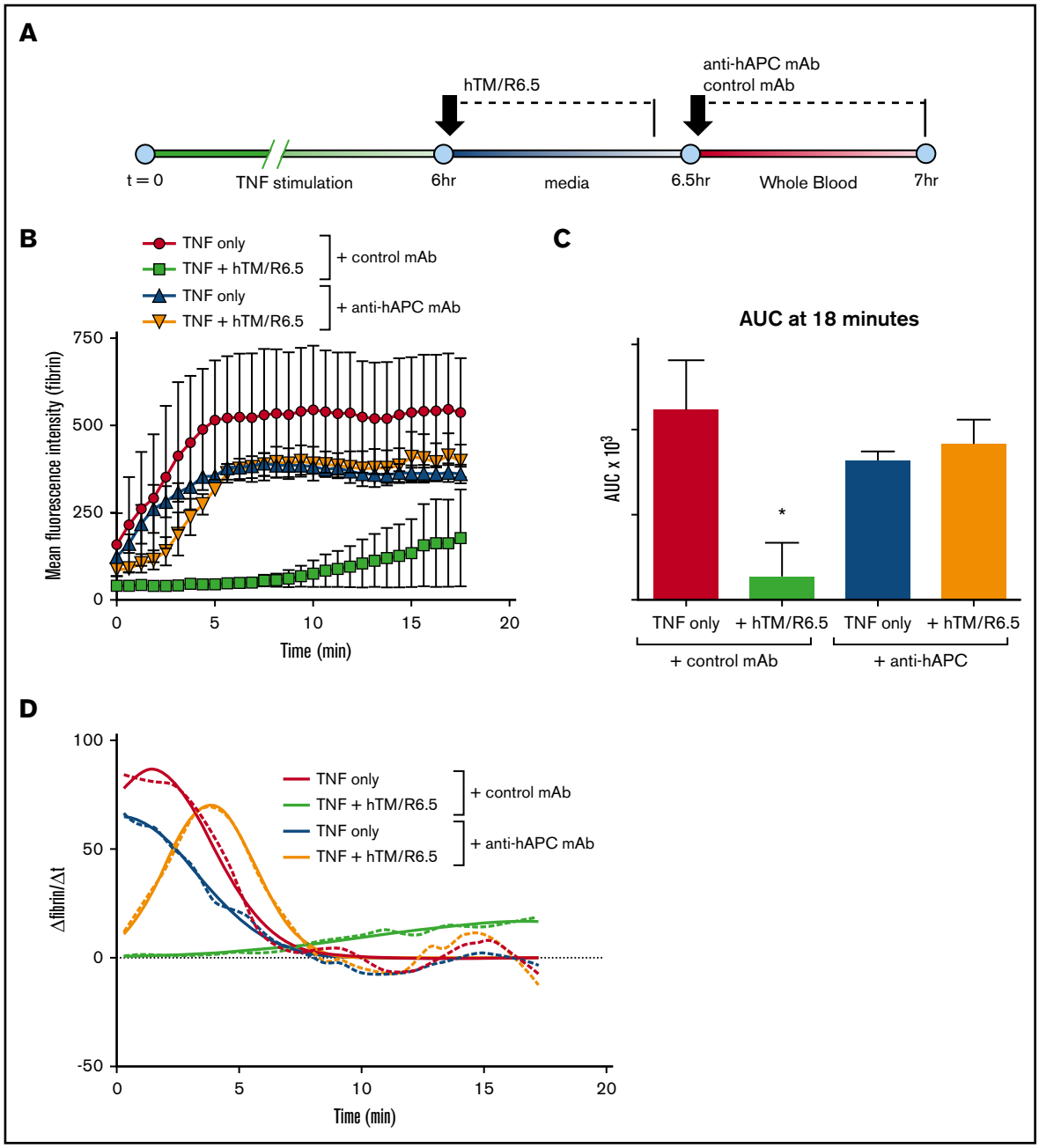

Figure 7. Antithrombotic activity of hTM/R6.5 is largely reversed by APC inhibition. (A) Design of APC inhibition experiments. Anti-hAPC antibody (HAPC1573) or equimolar isotype control were mixed into WB at 300 nM concentration. (B) Inhibition of APC significantly reduced the antithrombotic effect of hTM/R6.5 while not significantly affecting fibrin deposition in endothelialized channels not treated with fusion protein. Graph shows mean ± SEM, with n = 2 channels for each condition. (C) AUC analysis. *$P < .05$ vs all other conditions; #, not significant ($P = .47$); ##, not significant ($P = .72$). (D) Time curves of the first derivative of fibrin fluorescence intensity demonstrate the effects of various combinations of HAPC1573 and hTM/R6.5 on key parameters (described in supplemental Figure 4): peak fibrin generation rate and time to peak fibrin generation rate. Dotted lines show actual values, whereas solid lines show Gaussian functions fitted to these data. Parameters and their 95% confidence intervals are shown in supplemental Table 10.

permit recirculation, so exposure of endothelialized channels to WB flow was limited in duration by need to avoid cell settling and activation of the contact pathway (CTI provides ~1 hour of inhibition[34]). While our intention was to model TF-driven thrombosis, the use of CTI may likewise be viewed as a limitation, as it eliminates any contribution of factor XII–dependent coagulation, believed to play a role in certain systemic inflammatory syndromes.[59]

These limitations notwithstanding, the data presented provide several insights into the role of the endogenous PC pathway and the action of scFv/TM therapeutics. First, the contrasting results with inhibition and augmentation of endothelial TM suggest its importance in regulating coagulation under systemic inflammation. Second, the benefit of ICAM-targeted TM over its soluble counterpart supports the hypothesis that localization of the protein

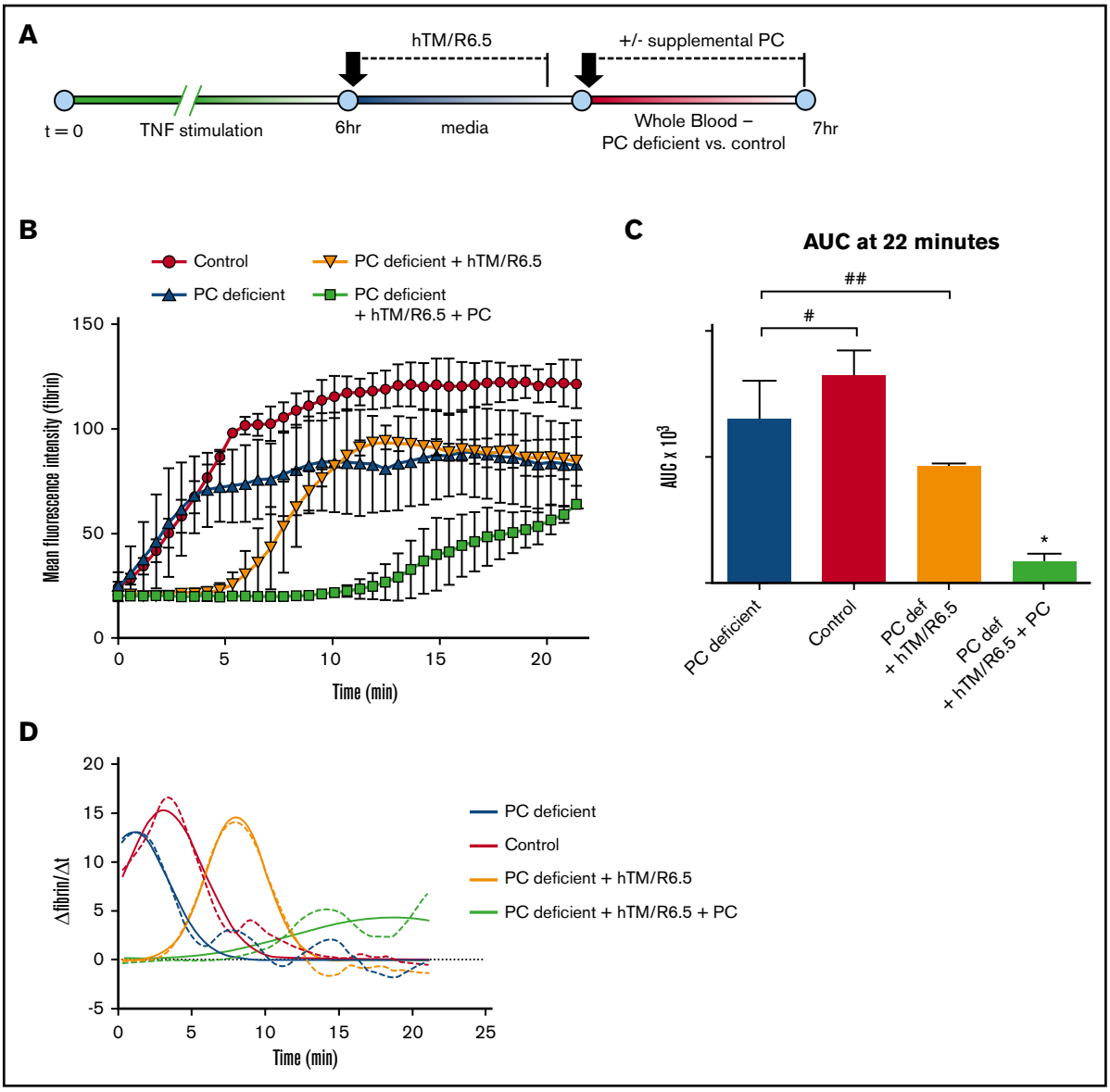

Figure 8. Antithrombotic activity of hTM/R6.5 is enhanced by PC supplementation in the setting of plasma PC deficiency. (A) Design of PC deficiency experiments. hTM/R6.5 was infused during the first 25 minutes of the TNF-α washout period, followed by infusion of PC-deficient blood vs control blood (prepared as described in Materials and methods). (B) The anti-thrombotic effect of hTM/R6.5 was reduced in PC-deficient blood and restored with the addition of supplemental PC. Graph shows mean ± SEM, with n = 2 channels for each condition. (C) AUC analysis. *$P < .05$ vs all other conditions; #, not significant ($P = .33$); ##, not significant ($P = .28$). (D) Time curves of the first derivative of fibrin fluorescence intensity demonstrate a delay in peak fibrin deposition but not a reduction in peak height by hTM/R6.5 in PC-deficient WB. Full efficacy is restored with the addition of supplemental plasma PC.

to the cellular membranes enhances its functional activity.[19,60,61] In fact, the difference in potency between these 2 agents may be more significant than their relative concentrations would suggest, as only a fraction of hTM/R6.5 molecules would have bound to the cell membrane. While ICAM-1 targeting of hTM/R6.5 was limited to hematopoietic and ECs in these studies, other cell types, such as epithelium, express ICAM-1, and may be both an important source of TF[24] and a valuable target of this approach.[62]

There are several reasons why binding of TM to cell membranes may enhance its antithrombotic activity. Cell-surface localization positions TM in proximity to TF and prothrombinase complexes assembled on cell membranes, resulting in immediate inhibition of thrombin and redirection to PC activation as it is produced.[63,64] Experiments involving antibody inhibition of APC and plasma PC deficiency suggest that PC activation is an important mechanism of hTM/R6.5 antithrombotic activity, as the ability of hTM/R6.5 to decrease the peak rate of fibrin generation was PC dependent. EC surface localization may accelerate activation of PC by partnering with endogenous EPCR, promoting PC cleavage by the thrombin/TM complex.[65] Although this was not investigated in the present studies, previous studies with the murine-specific analog of hTM/R6.5 demonstrated APC generation by cell-bound fusion

protein was inhibited when binding of PC to endothelial EPCR was blocked.[19]

The contribution of PC activation to the antithrombotic activity of hTM/R6.5 suggests a benefit with combination therapy, as pharmacologic replacement of TM alone may be insufficient in the setting of PC deficiency (as seen in septic patients[40,41]). While human plasma–derived PC concentrate failed to improve outcomes in sepsis or disseminated intravascular coagulation,[66,67] the synergy observed with pairing of PC and hTM/R6.5 suggests that simultaneous PC replacement and targeted delivery of TM may be an effective clinical strategy. Further investigation using patient specimens in our microfluidic model and confirmation in preclinical animal models will be necessary to determine if this combination therapy can surpass numerous previous pharmacologic attempts to prevent TF-driven inflammatory thrombosis and disseminated intravascular coagulation in the clinical setting.

Acknowledgments

This work was supported by a Center for Targeted Therapeutics and Translational Nanomedicine (CT^3N) Pilot Grant Award (ITMAT) at the University of Pennsylvania (C.F.G.). The work was also supported by National Institutes of Health, National Heart, Lung, and Blood Institute grants T32-HL007439 (C.F.G.), K08-HL130430 (C.F.G.), P01-HL040387 (M.P.), and R01-HL128398 (V.R.M.), and 7UM1-HL120877 (C.T.E.).

Authorship

Contribution: C.F.G., C.H.V., I.H.J., D.B.C., M.P., and V.R.M. conceived the study; C.F.G. and C.H.V. synthesized and purified recombinant proteins; C.F.G., I.H.J., C.H.V., and K.G. conducted the microfluidic experiments; I.H.J. performed confocal microscopy; C.F.G., C.H.V., and I.H.J. analyzed the data; and C.F.G., I.H.J., C.H.V., C.T.E., D.B.C., M.P., and V.R.M. wrote and edited the manuscript.

Conflict-of-interest disclosure: The authors declare no competing financial interests.

ORCID profiles: C.F.G., 0000-0001-9740-7672.

Correspondence: Vladimir R. Muzykantov, Perelman School of Medicine, University of Pennsylvania, STRC 10-178, 3400 Civic Center Blvd, Building 421, Philadelphia, PA 19104-5158; e-mail: muyzkant@mail.med.upenn.edu; and Mortimer Poncz, Children's Hospital of Philadelphia, ARC Room 317, 3615 Civic Center Blvd, Philadelphia, PA 19104; e-mail: poncz@e-mail.chop.edu.

References

1. Martinez-Cabriales S, Ocampo-Garza J, Barbosa-Moreno L, Chavez-Alvarez S, Ocampo-Candiani J. Purpura fulminans 10 years after contaminated cocaine use. *Lancet*. 2015;386(10004):e21.
2. Levi M. Recombinant soluble thrombomodulin: coagulation takes another chance to reduce sepsis mortality. *J Thromb Haemost*. 2015;13(4):505-507.
3. Fiusa MML, Carvalho-Filho MA, Annichino-Bizzacchi JM, De Paula EV. Causes and consequences of coagulation activation in sepsis: an evolutionary medicine perspective. *BMC Med*. 2015;13:105.
4. Foley JH, Conway EM. Cross talk pathways between coagulation and inflammation. *Circ Res*. 2016;118(9):1392-1408.
5. Engelmann B, Massberg S. Thrombosis as an intravascular effector of innate immunity. *Nat Rev Immunol*. 2013;13(1):34-45.
6. Allingstrup M, Wetterslev J, Ravn FB, Møller AM, Afshari A. Antithrombin III for critically ill patients. *Cochrane Database Syst Rev*. 2016;2:CD005370.
7. Martí-Carvajal AJ, Solà I, Gluud C, Lathyris D, Cardona AF. Human recombinant protein C for severe sepsis and septic shock in adult and paediatric patients. *Cochrane Database Syst Rev*. 2012;12:CD004388.
8. Jaimes F, De La Rosa G, Morales C, et al. Unfractioned heparin for treatment of sepsis: a randomized clinical trial (The HETRASE Study). *Crit Care Med*. 2009;37(4):1185-1196.
9. Zarychanski R, Abou-Setta AM, Kanji S, et al; Canadian Critical Care Trials Group. The efficacy and safety of heparin in patients with sepsis: a systematic review and metaanalysis. *Crit Care Med*. 2015;43(3):511-518.
10. Moore KL, Esmon CT, Esmon NL. Tumor necrosis factor leads to the internalization and degradation of thrombomodulin from the surface of bovine aortic endothelial cells in culture. *Blood*. 1989;73(1):159-165.
11. Boehme MW, Deng Y, Raeth U, et al. Release of thrombomodulin from endothelial cells by concerted action of TNF-alpha and neutrophils: in vivo and in vitro studies. *Immunology*. 1996;87(1):134-140.
12. MacGregor IR, Perrie AM, Donnelly SC, Haslett C. Modulation of human endothelial thrombomodulin by neutrophils and their release products. *Am J Respir Crit Care Med*. 1997;155(1):47-52.
13. Xu J, Qu D, Esmon NL, Esmon CT. Metalloproteolytic release of endothelial cell protein C receptor. *J Biol Chem*. 2000;275(8):6038-6044.
14. Gu J-M, Katsuura Y, Ferrell GL, Grammas P, Esmon CT. Endotoxin and thrombin elevate rodent endothelial cell protein C receptor mRNA levels and increase receptor shedding in vivo. *Blood*. 2000;95(5):1687-1693.
15. He X, Han B, Mura M, et al. Anti-human tissue factor antibody ameliorated intestinal ischemia reperfusion-induced acute lung injury in human tissue factor knock-in mice. *PLoS One*. 2008;3(1):e1527.
16. Witkowski M, Landmesser U, Rauch U. Tissue factor as a link between inflammation and coagulation. *Trends Cardiovasc Med*. 2016;26(4):297-303.
17. Vincent J-L, Ramesh MK, Ernest D, et al. A randomized, double-blind, placebo-controlled, phase 2b study to evaluate the safety and efficacy of recombinant human soluble thrombomodulin, ART-123, in patients with sepsis and suspected disseminated intravascular coagulation. *Crit Care Med*. 2013;41(9):2069-2079.

18. Greineder CF, Howard MD, Carnemolla R, Cines DB, Muzykantov VR. Advanced drug delivery systems for antithrombotic agents. *Blood*. 2013;122(9):1565-1575.

19. Greineder CF, Chacko A-M, Zaytsev S, et al. Vascular immunotargeting to endothelial determinant ICAM-1 enables optimal partnering of recombinant scFv-thrombomodulin fusion with endogenous cofactor. *PLoS One*. 2013;8(11):e80110.

20. Antoniak S, Mackman N. Tissue factor expression by the endothelium: coagulation or inflammation? *Trends Cardiovasc Med*. 2016;26(4):304-305.

21. Witkowski M, Rauch U. Tissue factor of endothelial origin: just another brick in the wall? *Trends Cardiovasc Med*. 2017;27(2):155-156.

22. Drake TA, Cheng J, Chang A, Taylor FB Jr. Expression of tissue factor, thrombomodulin, and E-selectin in baboons with lethal Escherichia coli sepsis. *Am J Pathol*. 1993;142(5):1458-1470.

23. Shaver CM, Grove BS, Clune JK, Mackman N, Ware LB, Bastarache JA. Myeloid tissue factor does not modulate lung inflammation or permeability during experimental acute lung injury. *Sci Rep*. 2016;6:22249.

24. Shaver CM, Grove BS, Putz ND, et al. Regulation of alveolar procoagulant activity and permeability in direct acute lung injury by lung epithelial tissue factor. *Am J Respir Cell Mol Biol*. 2015;53(5):719-727.

25. Pawlinski R, Wang J-G, Owens AP III, et al. Hematopoietic and nonhematopoietic cell tissue factor activates the coagulation cascade in endotoxemic mice. *Blood*. 2010;116(5):806-814.

26. Crikis S, Zhang XM, Dezfouli S, et al. Anti-inflammatory and anticoagulant effects of transgenic expression of human thrombomodulin in mice. *Am J Transplant*. 2010;10(2):242-250.

27. Raife TJ, Dwyre DM, Stevens JW, et al. Human thrombomodulin knock-in mice reveal differential effects of human thrombomodulin on thrombosis and atherosclerosis. *Arterioscler Thromb Vasc Biol*. 2011;31(11):2509-2517.

28. Smith CW, Rothlein R, Hughes BJ, et al. Recognition of an endothelial determinant for CD 18-dependent human neutrophil adherence and transendothelial migration. *J Clin Invest*. 1988;82(5):1746-1756.

29. Greineder CF, Hood ED, Yao A, et al. Molecular engineering of high affinity single-chain antibody fragment for endothelial targeting of proteins and nanocarriers in rodents and humans. *J Control Release*. 2016;226:229-237.

30. Lipowsky HH. Shear stress in the circulation. In Bevan J, Gabor K, and Gabor R, eds. Flow-Dependent Regulation of Vascular Function. New York, NY: Springer; 1995:28-45.

31. Tripodi A. Thrombin generation assay and its application in the clinical laboratory. *Clin Chem*. 2016;62(5):699-707.

32. Clark SR, Ma AC, Tavener SA, et al. Platelet TLR4 activates neutrophil extracellular traps to ensnare bacteria in septic blood. *Nat Med*. 2007;13(4):463-469.

33. Brinkmann V, Laube B, Abed UA, Goosmann C, Zychlinsky A. Neutrophil extracellular traps: how to generate and visualize them. *J Vis Exp*. 2010;(36):e1724.

34. Colace TV, Tormoen GW, McCarty OJT, Diamond SL. Microfluidics and coagulation biology. *Annu Rev Biomed Eng*. 2013;15:283-303.

35. Ikezoe T, Yang J, Nishioka C, et al. The fifth epidermal growth factor-like region of thrombomodulin exerts cytoprotective function and prevents SOS in a murine model. *Bone Marrow Transplant*. 2017;52(1):73-79.

36. Mohri M, Sugimoto E, Sata M, Asano T. The inhibitory effect of recombinant human soluble thrombomodulin on initiation and extension of coagulation: a comparison with other anticoagulants. *Thromb Haemost*. 1999;82(6):1687-1693.

37. Böhmer RH, Trinkle LS, Staneck JL. Dose effects of LPS on neutrophils in a whole blood flow cytometric assay of phagocytosis and oxidative burst. *Cytometry*. 1992;13(5):525-531.

38. Butenas S, Bouchard BA, Brummel-Ziedins KE, Parhami-Seren B, Mann KG. Tissue factor activity in whole blood. *Blood*. 2005;105(7):2764-2770.

39. Zhao X-Y, Yegneswaran S, Bauzon M, et al. Targeted inhibition of activated protein C anticoagulant activity by monoclonal antibody HAPC1573 for treatment of hemophilia [abstract]. *Blood*. 2016;128(22). Abstract 80.

40. Takahashi H, Takakuwa E, Yoshino N, Hanano M, Shibata A. Protein C levels in disseminated intravascular coagulation and thrombotic thrombocytopenic purpura: its correlation with other coagulation parameters. *Thromb Haemost*. 1985;54(2):445-449.

41. Fisher CJ Jr, Yan SB. Protein C levels as a prognostic indicator of outcome in sepsis and related diseases. *Crit Care Med*. 2000;28(9 Suppl):S49-S56.

42. Ware LB, Fang X, Matthay MA. Protein C and thrombomodulin in human acute lung injury. *Am J Physiol Lung Cell Mol Physiol*. 2003;285(3):L514-L521.

43. Coll E, Robles-Carrillo L, Reyes E, Francis JL, Amirkhosravi A. Assessment of protein C anticoagulant pathway by thrombin generation assay in the presence of endothelial cells. *J Thromb Haemost*. 2013;11(10):1916-1919.

44. Enlimomab Acute Stroke Trial Investigators. Use of anti-ICAM-1 therapy in ischemic stroke: results of the Enlimomab Acute Stroke Trial. *Neurology*. 2001;57(8):1428-1434.

45. Cosimi AB, Conti D, Delmonico FL, et al. In vivo effects of monoclonal antibody to ICAM-1 (CD54) in nonhuman primates with renal allografts. *J Immunol*. 1990;144(12):4604-4612.

46. Salmela K, Wramner L, Ekberg H, et al. A randomized multicenter trial of the anti-ICAM-1 monoclonal antibody (enlimomab) for the prevention of acute rejection and delayed onset of graft function in cadaveric renal transplantation: a report of the European Anti-ICAM-1 Renal Transplant Study Group. *Transplantation*. 1999;67(5):729-736.

47. Vuorte J, Lindsberg PJ, Kaste M, et al. Anti-ICAM-1 monoclonal antibody R6.5 (Enlimomab) promotes activation of neutrophils in whole blood. *J Immunol*. 1999;162(4):2353-2357.

48. Zheng Y, Chen J, Craven M, et al. In vitro microvessels for the study of angiogenesis and thrombosis. *Proc Natl Acad Sci USA*. 2012;109(24):9342-9347.

49. Tsai M, Kita A, Leach J, et al. In vitro modeling of the microvascular occlusion and thrombosis that occur in hematologic diseases using microfluidic technology. *J Clin Invest*. 2012;122(1):408-418.

50. Tourovskaia A, Fauver M, Kramer G, Simonson S, Neumann T. Tissue-engineered microenvironment systems for modeling human vasculature. *Exp Biol Med (Maywood)*. 2014;239(9):1264-1271.

51. Esch EW, Bahinski A, Huh D. Organs-on-chips at the frontiers of drug discovery. *Nat Rev Drug Discov*. 2015;14(4):248-260.

52. Roberts MA, Kotha SS, Phong KT, Zheng Y. Micropatterning and assembly of 3D microvessels. *J Vis Exp*. 2016;(115):e54457.

53. Carnemolla R, Villa CH, Greineder CF, et al. Targeting thrombomodulin to circulating red blood cells augments its protective effects in models of endotoxemia and ischemia-reperfusion injury. *FASEB J*. 2017;31(2):761-770.

54. Villa CH, Pan DC, Zaitsev S, Cines DB, Siegel DL, Muzykantov VR. Delivery of drugs bound to erythrocytes: new avenues for an old intravascular carrier. *Ther Deliv*. 2015;6(7):795-826.

55. Fuentes RE, Zaitsev S, Ahn HS, et al. A chimeric platelet-targeted urokinase prodrug selectively blocks new thrombus formation. *J Clin Invest*. 2016; 126(2):483-494.

56. Polacheck WJ, Li R, Uzel SGM, Kamm RD. Microfluidic platforms for mechanobiology. *Lab Chip*. 2013;13(12):2252-2267.

57. Lupu C, Westmuckett AD, Peer G, et al. Tissue factor-dependent coagulation is preferentially up-regulated within arterial branching areas in a baboon model of Escherichia coli sepsis. *Am J Pathol*. 2005;167(4):1161-1172.

58. Antoniak S, Mackman N. Letter to Editor response: endothelial cell tissue factor and coagulation. *Trends Cardiovasc Med*. 2017;27(2):157.

59. Nickel KF, Long AT, Fuchs TA, Butler LM, Renné T. Factor XII as a therapeutic target in thromboembolic and inflammatory diseases. *Arterioscler Thromb Vasc Biol*. 2017;37(1):13-20.

60. Ding B-S, Hong N, Christofidou-Solomidou M, et al. Anchoring fusion thrombomodulin to the endothelial lumen protects against injury-induced lung thrombosis and inflammation. *Am J Respir Crit Care Med*. 2009;180(3):247-256.

61. Greineder CF, Brenza JB, Carnemolla R, et al. Dual targeting of therapeutics to endothelial cells: collaborative enhancement of delivery and effect. *FASEB J*. 2015;29(8):3483-3492.

62. Tosi MF, Stark JM, Smith CW, Hamedani A, Gruenert DC, Infeld MD. Induction of ICAM-1 expression on human airway epithelial cells by inflammatory cytokines: effects on neutrophil-epithelial cell adhesion. *Am J Respir Cell Mol Biol*. 1992;7(2):214-221.

63. Stern D, Nawroth P, Handley D, Kisiel W. An endothelial cell-dependent pathway of coagulation. *Proc Natl Acad Sci USA*. 1985;82(8):2523-2527.

64. Ivanciu L, Krishnaswamy S, Camire RM. New insights into the spatiotemporal localization of prothrombinase in vivo. *Blood*. 2014;124(11):1705-1714.

65. Stearns-Kurosawa DJ, Kurosawa S, Mollica JS, Ferrell GL, Esmon CT. The endothelial cell protein C receptor augments protein C activation by the thrombin-thrombomodulin complex. *Proc Natl Acad Sci USA*. 1996;93(19):10212-10216.

66. Esmon CT. Role of coagulation inhibitors in inflammation. *Thromb Haemost*. 2001;86(1):51-56.

67. Manco-Johnson MJ, Bomgaars L, Palascak J, et al. Efficacy and safety of protein C concentrate to treat purpura fulminans and thromboembolic events in severe congenital protein C deficiency. *Thromb Haemost*. 2016;116(1):58-68.